



## Full paper/Mémoire

# Silver(I) thiosemicarbazone complex $[Ag(catcsc)(PPh_3)_2]NO_3$ : Synthesis, characterization, crystal structure, and antibacterial study

Aliakbar Dehno Khalaji <sup>a,\*</sup>, Ensieh Shahsavani <sup>b</sup>, Nourollah Feizi <sup>b</sup>,  
Monika Kucerakova <sup>c</sup>, Michal Dusek <sup>c</sup>, Raouf Mazandarani <sup>d</sup>

<sup>a</sup> Department of Chemistry, Faculty of Science, Golestan University, Gorgan, Iran

<sup>b</sup> Department of Chemistry, Payame Noor University, Mashhad, Iran

<sup>c</sup> Institute of Physics of the Czech Academy of Sciences, Na Slovance 2, 182 21 Prague 8, Czech Republic

<sup>d</sup> Department of Biology, Faculty of Science, Golestan University, Gorgan, Iran

## ARTICLE INFO

## Article history:

Received 8 June 2016

Accepted 5 September 2016

Available online xxxx

## Keywords:

Silver(I) complex

Single-crystal

Antibacterial effect

Tetrahedral

Bidentate

## ABSTRACT

We report the synthesis, characterization and crystal structure of a new mononuclear silver(I) complex,  $[Ag(catcsc)(PPh_3)_2]NO_3$  ( $catcsc = 3$ -phenylpropenalthiosemicarbazone). The complex was prepared by the reaction of  $catcsc$  and  $AgNO_3$  in the presence of  $PPh_3$  and characterized by elemental analysis (CHN), FTIR,  $^1H$ ,  $^{13}C$  and  $^{31}P$  NMR spectroscopy, and single-crystal X-ray diffraction. In the complex,  $catcsc$  acts as a bidentate NS ligand while the nitrate is a counter ion. The silver ion is coordinated by a bidentate ligand and two  $PPh_3$  in the form of a distorted tetrahedron. In addition, the antibacterial effect of the complex was studied against the standard strains of two gram-positive (*Staphylococcus aureus* and *Enterococcus faecalis*) and two gram-negative (*Escherichia coli* and *Pseudomonas aeruginosa*) bacteria.

© 2016 Académie des sciences. Published by Elsevier Masson SAS. All rights reserved.

## 1. Introduction

Thiosemicarbazone compounds, an important class of N,S-donor ligands, have been studied for their structural diversity [1,2] and chemical properties [2]. Thiosemicarbazones can bind to a metal center in various coordination modes in their anionic as well as neutral forms [3–6]. Their complexes with transition metals have a large range of biological applications as antibacterial [3], anti-tumor [4] and anticancer [5] agents. The less investigated copper(I) and silver(I) complexes can also form mono-, di- and poly-nuclear compounds with interesting structural features [7–10]. Here thiosemicarbazones usually act as monodentate ligands bonding through the sulfur atoms [7,8], but in the literature there are also sporadic reports on

copper(I) [9] and silver(I) [10] complexes with chelating N,S thiosemicarbazones.

In continuation of our research of transition metal complexes with thiosemicarbazone ligands [11–13], in this paper we report the synthesis, spectroscopic characterization, crystal structure, thermal studies and antibacterial activities of a new mononuclear silver(I) thiosemicarbazone complex  $[Ag(catcsc)(PPh_3)_2]NO_3$  (Scheme 1).

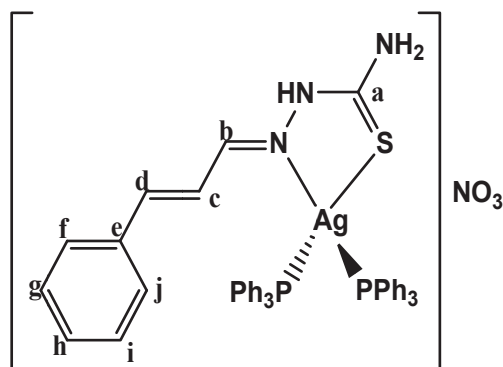
## 2. Experimental

## 2.1. Materials and methods

$AgNO_3$ ,  $PPh_3$ , cinnamaldehyde, thiosemicarbazide, ethanol and acetonitrile were purchased from Merck and used as received. The thiosemicarbazone ligand  $catcsc$  was prepared in high yield following a literature procedure [14]. Infrared spectra were recorded using a KBr disk on an FTIR

\* Corresponding author.

E-mail address: alidkhalaji@yahoo.com (A. Dehno Khalaji).



**Scheme 1.** The chemical structure of  $[Ag(catcsc)(PPh_3)_2]NO_3$ .

(Perkin–Elmer) spectrometer. Elemental analyses were carried out using a Heraeus CHN–O–Rapid analyzer.  $^1H$ ,  $^{13}C$  and  $^{31}P$  NMR spectra were measured on a Bruker DRX-400 AVANCE spectrometer at 400 MHz. All chemical shifts were reported in  $\delta$  units downfield from TMS. The TG was performed on a PerkinElmer TGA/DTA lab system 1 (Technology by SII) in an argon atmosphere, using the heating rate  $20^\circ C/min$  and the temperature span  $30–750^\circ C$ . UV–vis spectra were recorded by a PerkinElmer Spectrometer Lambda 25.

## 2.2. Preparation of $[Ag(catcsc)(PPh_3)_2]NO_3$

The ligand catcsc (0.021, 1 mmol) was added to an acetonitrile suspension of  $AgNO_3$  (0.017 g, 0.1 mmol) and  $PPh_3$  (0.052 g, 0.2 mmol) (molar ratio, 1:2) and stirred for 0.5 h until a yellow clear solution was obtained. The solution was left at  $-4^\circ C$  for several days and then slowly evaporates at room temperature. The white polygon crystals were filtered and washed twice with acetonitrile, and dried at room temperature. Anal. Calcd for  $C_{46}H_{41}AgN_4O_3P_2S$ : C, 61.41; H, 4.59; N, 6.23; S, 3.56%. Found: C, 61.47; H, 4.65; N, 6.31; S, 3.52%. FTIR data (KBr,  $cm^{-1}$ ):  $\nu$  (N–H) 3143 (–NH<sub>2</sub> group), 3251–3409,  $\nu$  (C–H aromatic) 3017,  $\nu$  (C–H imine) 2979,  $\nu$  (–C=N– imine) 1562,  $\{\nu(C-C) + \nu(C-N) + \nu(P-C_{Ph})\}$  993, 1056, 1148, 1182,  $\nu$  (C=S) 814.  $^1H$  NMR (DMSO- $d_6$ ,  $\delta$  ppm): 11.7 (s, 1H, –NH–), 8.6 (s, 1H, –C<sup>b</sup>H = N–), 8.0–8.1 (d, 1H, C<sup>h</sup>H); 7.8 (s, 2H, –NH<sub>2</sub>); 7.2–7.6 (32H,  $PPh_3$  + C<sup>c,d</sup>H); 7.0–7.1 (d, 2H, C<sup>f,j</sup>H); 6.8 (dd, 2H, C<sup>g,i</sup>H).  $^{13}C$  NMR (DMSO- $d_6$ ,  $\delta$  ppm): 175.7 (C<sup>a</sup>=S), 147.5 (C<sup>b</sup> = N), 124.8–140.7 (C<sup>c-j</sup> +  $PPh_3$ ).  $^{31}P$  NMR (DMSO- $d_6$ ,  $\delta$  ppm): 7.6. UV–vis ( $\lambda_{max}$ , nm): 272, 372.

## 2.3. X-ray crystallography

A single crystal of  $[Ag(catcsc)(PPh_3)_2]NO_3$  of size  $0.09\text{ mm} \times 0.07\text{ mm} \times 0.06\text{ mm}$  was selected for an X-ray diffraction study. Crystallographic measurements were done at 293 K with a four circle CCD diffractometer Gemini of Oxford diffraction, Ltd., with mirrors-collimated Cu  $K\alpha$  radiation ( $\lambda = 1.54184\text{ \AA}$ ). Although the quality of the single crystals was low (as indicated by the  $R_{int}$  factor in Table 2 for merging symmetry equivalent reflections) the crystal structure could be nevertheless easily solved by charge flipping with program SUPERFLIP [15] and refined with the

Jana2006 program package [16] by the full-matrix least-squares technique on  $F^2$ . The molecular structure plots were prepared by using Diamond 4 [17]. Hydrogen atoms were mostly discernible in difference Fourier maps and could be refined to reasonable geometry. According to the common practice, hydrogen atoms attached to carbons were kept in ideal positions during the refinement. The isotropic atomic displacement parameters of hydrogen atoms were set to  $1.2 U_{eq}$  of their hydrogen atoms. Crystallographic data and details of the data collection and structure solution and refinements are listed in Table 1.

## 2.4. Antibacterial activity

The antibacterial activity of the catcsc ligand and its silver(I) complex  $[Ag(catcsc)(PPh_3)_2]NO_3$  were investigated against two standard strains of gram-positive (*Staphylococcus aureus* ATCC-25923 and *Enterococcus faecalis* ATCC-29212) and gram-negative (*Escherichia coli* ATCC 25922 and *Pseudomonas aeruginosa* ATCC-27853) bacteria by the pure plate method. The tests were performed by using the methodology described in the guidelines of the 'Comité de l'antibiogramme' de la 'Société française de microbiologie' (CA-SFM, [www.sfm.asso.fr](http://www.sfm.asso.fr)) [18]. A solution of catcsc and its complex were prepared at 20 mg/mL in DMSO under sterile conditions. After dilution, 10 petri plates with 10, 20, 30, 40, 50, 60, 70, 80, 90 and 100  $\mu g/mL$  concentration of catcsc and its complex were prepared. About  $2 \times 10^4$  bacteria suspended in sterile distilled water were inoculated on the different petri plates. After incubation for 24 h at  $37^\circ C$ , the minimum inhibitory concentration (MICs  $\mu g/mL$ ) was determined.

## 3. Results and discussion

### 3.1. Synthesis and characterization

Thiosemicarbazone ligand catcsc was prepared in high yield using a standard method [14]. The ligand catcsc was

**Table 1**  
Crystallographic and refinement data for  $[Ag(catcsc)(PPh_3)_2]NO_3$ .

Empirical formula	$C_{46}H_{41}AgN_4O_3P_2S$
Formula weight	899.75
Crystal system	Orthorhombic
Space group	$P2_12_12_1$
$a/\text{\AA}$	12.2631(4)
$b/\text{\AA}$	23.3682(6)
$c/\text{\AA}$	28.6672(9)
$V/\text{\AA}^3$	8215.1(4)
$Z$	2
$\mu/\text{mm}^{-1}$	5.52
$T/K$	293
Crystal size/mm	$0.09 \times 0.07 \times 0.06$
$T_{min}$	0.881
$T_{max}$	1
Measured reflections	47,513
Independent reflections	14,424
Reflections with $I > 3\sigma(I)$	10,972
$R[F^2 > 3\sigma(F^2)]$	0.043
$wR(F^2)$	0.053
$S, R_{int}$	1.52, 0.084
Parameters	1045
$\Delta\rho_{max,min}/e\text{\AA}^{-3}$	0.32, –0.28

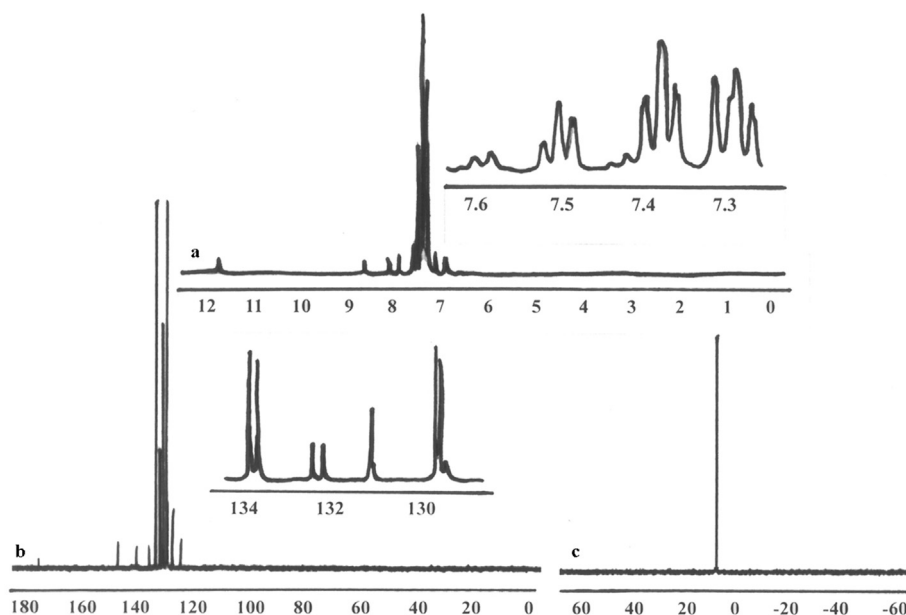
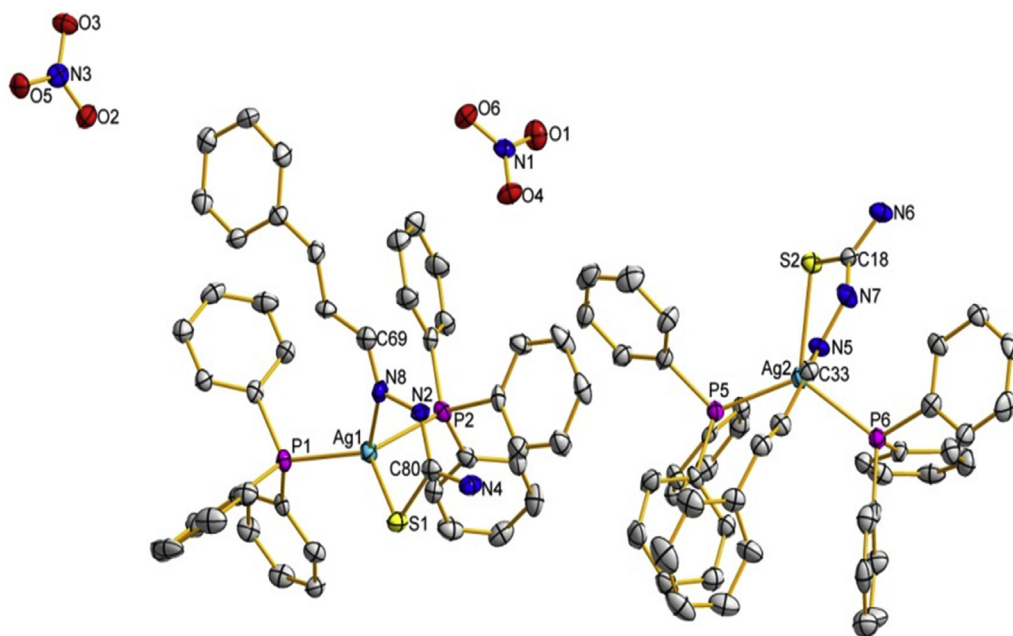


Fig. 1. a)  $^1\text{H}$ , b)  $^{13}\text{C}$  and c)  $^{31}\text{P}$  NMR spectrum of  $[\text{Ag}(\text{catssc})(\text{PPh}_3)_2]\text{NO}_3$ .

added to an acetonitrilic suspension of  $\text{AgNO}_3$  and  $\text{PPh}_3$  (molar ratio, 1:2) and was stirred for 0.5 h to obtain the silver(I) complex  $\{[\text{Ag}(\text{catssc})(\text{PPh}_3)_2]\text{NO}_3\}$ . Suitable crystals of  $[\text{Ag}(\text{catssc})(\text{PPh}_3)_2]\text{NO}_3$  were prepared by slow evaporation of solvent at 273 K, and characterized by elemental analysis (CHNS), FTIR, UV–vis,  $^1\text{H}$ ,  $^{13}\text{C}$  and  $^{31}\text{P}$  NMR spectroscopy, thermogravimetric analysis and single-crystal X-ray diffraction. Elemental analysis revealed that the ratio of

$\text{Ag}$ ,  $\text{catssc}$  and  $\text{PPh}_3$  in  $[\text{Ag}(\text{catssc})(\text{PPh}_3)_2]\text{NO}_3$  is 1:1:2. The stability of the complex in solution at room temperature is low, but the complex is stable as a solid for several months. The solubility of the complex depends on the solvent used. Thus, the complex is only slightly soluble in common organic solvents such as  $\text{C}_2\text{H}_5\text{OH}$ ,  $\text{CHCl}_3$ ,  $\text{CH}_3\text{CN}$ , but it is well soluble in coordinated solvents such as DMF and DMSO.



**Table 2**Selected bond distances (Å) and angles of  $[\text{Ag}(\text{catsc})(\text{PPh}_3)_2]\text{NO}_3$ .

Ag1 N8	2.480(6)	N5 C33	1.288(7)	N4 C80	1.320(8)
Ag2 N5	2.468(5)	Ag2 P6	2.4951(16)	N2 N8	1.370(7)
Ag1 S1	2.6124(16)	N8 C69	1.287(7)	N2 C80	1.337(8)
Ag1 P1	2.4354(15)	N7 C18	1.349(8)	S1 C80	1.702(6)
Ag1 P2	2.4996(16)	Ag2 P5	2.4406(15)	S2 C18	1.706(6)
Ag2 S2	2.6085(15)	N6 C18	1.329(8)	N5 N7	1.384(7)
N8 Ag1 S1	71.87(5)	N8 Ag1 P1	118.17(5)	N8 Ag1 P2	96.72(5)
N5 Ag1 S2	72.80(5)	N5 Ag1 P5	119.98(5)	N5 Ag1 P6	96.57(5)
S1 Ag1 P1	120.18(5)	N6 C18 N7	116.0(5)	N8 N2 C80	121.4(5)
S1 Ag1 P2	111.45(5)	N5 C33 C44	120.8(5)	O1 N1 O4	121.5(5)
P1 Ag1 P2	123.91(5)	N8 C69 C39	122.1(5)	O2 N3 O3	121.3(5)
N8 Ag1 P1	118.17(5)	S1 C80 N2	123.0(5)	N7 N5 C33	114.5(5)
N8 Ag1 P2	96.72(5)	S1 C80 N4	121.2(5)	N5 N7 C18	121.9(5)
N8 Ag1 S1	71.87	N2 C80 N4	115.7(5)	N2 N8 C69	115.4(5)
S2 Ag2 P5	114.64(5)	Ag1 S1 C80	95.8(2)	S2 C18 N6	121.4(5)
S2 Ag2 P6	116.67(5)	Ag2 S2 C18	98.4(2)	S2 C18 N7	122.5(5)
P5 Ag2 P6	123.52(5)				

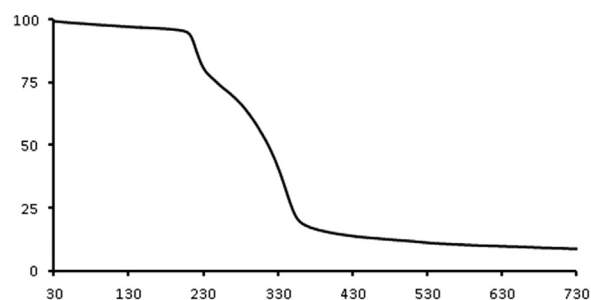
**Table 3**

Selected parameters of the hydrogen bonds involving the nitrate ions.

Hydrogen bonding	D–H (Å)	H...A (Å)	D...A (Å)	D–H...A (°)
N7 H1n7 O6	0.73(7)	2.07(7)	2.777(7)	164(8)
N2 H1n2 O5	0.88(5)	1.97(5)	2.790(7)	155(5)
N4 H1n4 O6	0.94(7)	2.00(7)	2.891(7)	159(6)
N4 H2n4 O3	0.73(7)	2.37(7)	3.024(7)	149(7)
N6 H1n6 O4	0.83(7)	2.11(7)	2.916(7)	165(7)
N6 H2n6 O5	0.94(7)	2.02(7)	2.904(7)	157(6)

### 3.2. FTIR spectroscopy

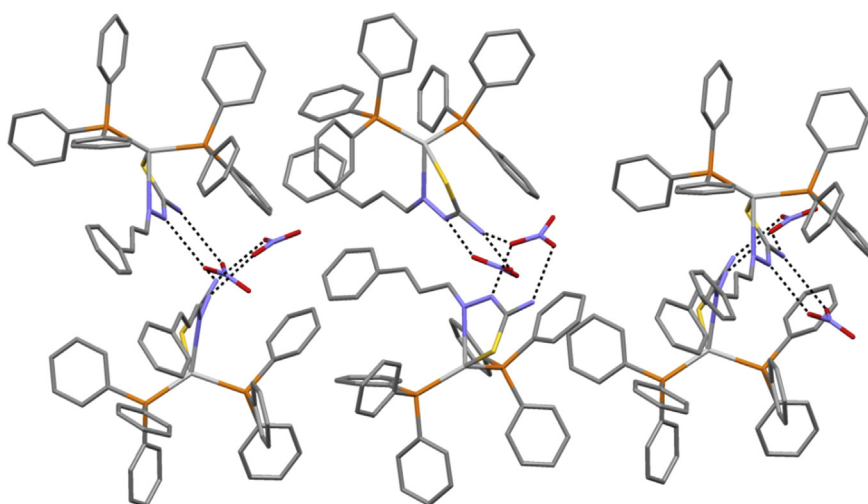
The FTIR spectrum of  $[\text{Ag}(\text{catsc})(\text{PPh}_3)_2]\text{NO}_3$  showed three bands in the range of 3251 and 3409  $\text{cm}^{-1}$  (due to  $-\text{NH}_2$ ) and 3143  $\text{cm}^{-1}$  (due to  $-\text{NH}-$ ). Appearance of the characteristic bands of  $\nu(\text{C}=\text{S})$  and  $\nu(\text{C}=\text{N})$  vibrational modes at 814 and 1562  $\text{cm}^{-1}$  respectively, indicates the presence of the catsc ligand. Shifting of  $\nu(\text{C}=\text{S})$  and  $\nu(\text{C}=\text{N})$  bands to lower energy in the complex compared to the free

**Fig. 4.** The TG curve of  $[\text{Ag}(\text{catsc})(\text{PPh}_3)_2]\text{NO}_3$ .

ligand (850 and 1624  $\text{cm}^{-1}$ , respectively) confirmed that the catsc ligand was coordinated to silver(I) by S,N-donor atoms. The  $\nu(\text{P}-\text{C}_{\text{ph}})$  bands were found at 1056  $\text{cm}^{-1}$ , indicating coordination of  $\text{PPh}_3$  via the P atom to the silver(I) ion [19]. The  $\nu(\text{C}-\text{H}$  aromatic) and  $\nu(\text{C}-\text{H}$  iminic) stretching frequency of catsc and  $\text{PPh}_3$  appeared at 3017 and 2979  $\text{cm}^{-1}$ , respectively. Finally, the  $\nu(\text{N}-\text{O})$  asymmetric stretching mode of the nitrate anion appeared at 1390  $\text{cm}^{-1}$  [20].

### 3.3. $^1\text{H}$ , $^{13}\text{C}$ and $^{31}\text{P}$ NMR spectroscopy

$^1\text{H}$ ,  $^{13}\text{C}$  and  $^{31}\text{P}$  NMR spectra were recorded using  $\text{DMSO}-d_6$  (Fig. 1). The  $^1\text{H}$  NMR spectrum exhibited a singlet signal of the  $\text{N}-\text{NH}-\text{C}$  at about 11.7 ppm, which indicated that the coordination of the catsc ligand to the silver(I) ion is in its neutral form, via N,S-donor atoms [10,19]. Another singlet signal at 8.6 ppm revealed the presence of the iminic hydrogen ( $-\text{CH}=\text{N}-$ ). The protons of the  $\text{PPh}_3$  and  $-\text{NH}_2$  groups and of the ethylenic hydrogen ( $\text{C}^{\text{d}}\text{H}$ ) appeared in the range of 7.1–7.6 and 8–8.1 ppm (m, 34H). The signals of  $\text{C}^{\text{i-g}}\text{H}$  and  $\text{C}^{\text{j-f}}\text{H}$  protons appeared at 6.8 (dd, 2H,  $J^1 = 16$  Hz,  $J^2 = 9.6$  Hz) and 7–7.1 (d, 2H,  $J = 16$  Hz), respectively. A doublet signal at 7.8 ppm ( $J = 9.6$  Hz) was related to the  $\text{C}^{\text{h}}\text{H}$  proton. The  $^{13}\text{C}$  NMR spectrum showed two signals at 175.7

**Fig. 3.** The hydrogen bonds between cationic complexes and nitrate anion.



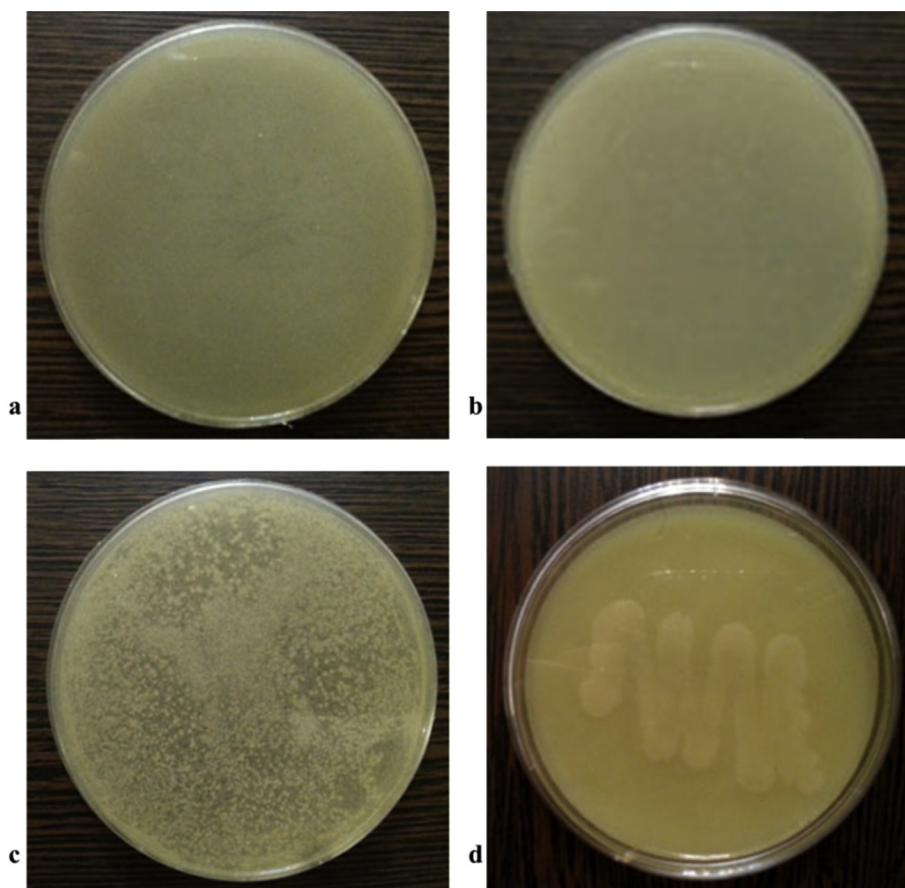


Fig. 5. The antibacterial screening of the complex with the 50  $\mu\text{g/mL}$  concentration against (a) *S. aureus*, (b) *E. faecalis*, (c) *E. coli* and (d) *P. aeruginosa*.

and 147.5 ppm for carbon atoms of  $\text{C}^{\text{a}}=\text{S}$  and  $\text{C}^{\text{b}}=\text{N}$ , respectively [21], while the  $\text{C}^{\text{c-j}}$  carbons and the carbons of two  $\text{PPh}_3$  appeared at 124.8–140.7 and 136.1 ppm. The aromatic carbons of catsc and  $\text{PPh}_3$  appeared at 124.8–133.8 ppm. The presence of only one signal in the  $^{31}\text{P}$  NMR spectrum of the complex at 7.6 ppm confirmed that the chemical environment of two P atoms is similar and the geometry around the silver(I) ion must be tetrahedral, not square-planar [10,19].

### 3.4. UV–vis spectroscopy

The UV–vis spectra were obtained in DMSO solution. The catsc ligand showed two bands corresponding to  $n \rightarrow \pi^*$  (367 nm) and  $\pi \rightarrow \pi^*$  (342 nm) transitions, related to azomethine and thioamide functions. In the UV–vis spectrum of  $[\text{Ag}(\text{catsc})(\text{PPh}_3)_2]\text{NO}_3$ ,  $n \rightarrow \pi^*$  and  $\pi \rightarrow \pi^*$  transitions exhibited the red (372 nm) and blue (272 nm) shifts, respectively, as a result of coordination.

### 3.5. Crystal structure

The complex  $[\text{Ag}(\text{catsc})(\text{PPh}_3)_2]\text{NO}_3$  crystallized in an orthorhombic crystal system with space group  $P2_12_12_1$ . Its molecular structure is shown in Fig. 2; selected bond

distances and angles are presented in Table 2. The complex is formed by two symmetry-independent cationic molecules and two nitrate counter anions. The silver(I) ion is coordinated to two different P atoms from two  $\text{PPh}_3$  molecules and two S and N atoms of the thiosemicarbazone ligand catsc in its neutral form. The Ag–N, Ag–S and Ag–P bond distances lie in ranges 2.468(5)–2.480(6), 2.608(5)–2.612(6) and 2.435(4)–2.499(8) Å, respectively. All of these bonds are similar to those in already reported mononuclear silver(I) thiosemicarbazone complexes [10]. The bond angles around the silver(I) ions are in the range of ca. 71.87(8)–123.91(7)°, corresponding to strongly distorted tetrahedral geometry similar to that found for copper(I) thiosemicarbazone complexes [22,23]. The distortion of the tetrahedral geometry is caused by the bulky  $\text{PPh}_3$  ligands

Table 4  
The MIC of catsc and  $[\text{Ag}(\text{catsc})(\text{PPh}_3)_2]\text{NO}_3$ .

Species of bacteria	MIC of complex ( $\mu\text{g/mL}$ )	MIC of catsc ligand ( $\mu\text{g/mL}$ )
<i>E. faecalis</i> (ATCC29212)	60	>500
<i>S. aureus</i> (ATCC25923)	<1	>500
<i>E. coli</i> (ATCC25922)	<1	>500
<i>P. aeruginosa</i> (ATCC2753)	>500	>500

and by the pressure angle of the chelating ligand arising from the fact that the S1 atom and hydrazinic nitrogen N8 are in the Z position with respect to the C8–N2 bond in the complex [22,23]. Normally, catsc is ready to be coordinated to the silver(I) ion through S and hydrazinic nitrogen atoms with the formation of a five-membered metallocycle [22]. The coordination of catsc to the silver(I) ion as a bidentate ligand causes the change of the configuration from E in the free ligand to Z in the complex. The S=C bond distances lie in the range 1.702(5)–1.706(6) Å and are also close to those observed in similar complexes [19,20]. Also, the coordination of the catsc ligand to silver(I) by N and S atoms causes decreasing of the C=S double bond distance in the complex as compared to the free ligand. In addition, there are several intermolecular hydrogen bonds in the complex between oxygen atoms of nitrate anions and hydrogen atoms of the NH<sub>2</sub> group or H-hydrazinic atoms of the catsc ligand (Table 3, Fig. 3).

### 3.6. Thermal gravimetry

To examine the thermal stability of [Ag(catsc)(PPh<sub>3</sub>)<sub>2</sub>]NO<sub>3</sub>, thermal gravimetry (TG) was carried out between 30 and 730 °C under argon flow (Fig. 4). The compound [Ag(catsc)(PPh<sub>3</sub>)<sub>2</sub>]NO<sub>3</sub> is stable up to about 200 °C. Decomposition in two stages occurs between 200 and 430 °C with a mass loss of 85%. At the first stage (200–230 °C), the complex shows a mass loss of about 28% due to the partial decomposition, while in the second stage (230–430 °C), the complex loses 57% of the mass, leaving Ag as the final product.

### 3.7. Antibacterial effects

The minimum inhibitory concentrations (MICs) of the catsc ligand and its silver(I) complex against two standard strains of gram-positive (*S. aureus* ATCC-25923 and *E. faecalis* ATCC-29212) and gram-negative (*E. coli* ATCC 25922 and *P. aeruginosa* ATCC-27853) bacteria are shown in Fig. 5 and presented in Table 4. The results showed that at 500 µg/mL catsc has no antibacterial activity against any of the tested bacteria [23]. The complex is inactive against *P. aeruginosa* at the 500 µg/mL concentration, but it is active against *S. aureus*, *E. faecalis* and *E. coli*, with better activity against *S. aureus* than against *E. faecalis*. The considerably higher antibacterial activity of the complex compared with the free ligand, especially towards gram-positive bacteria, has been also observed for the similar copper(I) thiosemicarbazone complex [23]. The differences of MICs found for the ligand and for the complex are due to its ability to penetrate cells walls, which is structure dependent [24].

## 4. Conclusions

A new mononuclear silver(I) thiosemicarbazone complex [Ag(catsc)(PPh<sub>3</sub>)<sub>2</sub>]NO<sub>3</sub> has been synthesized and characterized. Single crystal structure determination shows that the central silver(I) ion coordinate with two P atoms from two PPh<sub>3</sub> molecules, and with S and N atoms of the catsc ligand. The silver(I) ion adopts a distorted tetrahedral

geometry. The antibacterial activity of [Ag(catsc)(PPh<sub>3</sub>)<sub>2</sub>]NO<sub>3</sub> is enhanced with respect to the free ligand.

## Acknowledgements

We are grateful to the Payame Noor University and Golestan University for financial support of this work. Structure analysis was supported by the project 15-12653S of the Czech Science Foundation using instruments of the ASTRA lab established within the Operation program Prague Competitiveness – project CZ.2.16/3.1.00/2451.

## Supplementary data

Crystallographic data (excluding structure factors) for the structure reported in this paper have been deposited with the Cambridge Crystallographic Center, CCDC No. 1501507. Copies of the data can be obtained free of charge at <http://www.ccdc.cam.ac.uk>.

## References

- [1] M. Serda, D.S. Kalinowski, A. Mrozek-Wilczkiewicz, R. Musiol, A. Szurko, A. Ratuszna, N. Pantarat, Z. Kovacevic, A.M. Merlot, D.R. Richardson, J. Polanski, Bioorg. Med. Chem. Lett. 22 (2012) 5527–5531.
- [2] A.D. Khalaji, G. Grivani, S. Jalali Akerdi, K. Gotoh, H. Ishida, H. Mighani, Struct. Chem. 21 (2010) 995–1003.
- [3] U. El-Ayaan, M.M. Youssef, S. Al-Shihry, J. Mol. Struct. 936 (2009) 213–219.
- [4] D. Kovala-Demertzi, A. Alexandratos, A. Papageorgiou, P.N. Yadav, P. Dalezis, M.A. Demertzis, Polyhedron 27 (2008) 2731–2738.
- [5] S. Chandra, Vandana, Spectrochim. Acta, Part A 129 (2014) 333–338.
- [6] M.X. Li, C.L. Chen, D. Zhang, J.Y. Niu, B.S. Ji, Eur. J. Med. Chem. 45 (2010) 3169–3177.
- [7] T.S. Lobana, R. Sharma, G. Hundal, A. Castineiras, R.J. Butcher, Polyhedron 47 (2012) 134–142.
- [8] T.S. Lobana, S. Khanna, G. Hundal, R.J. Butcher, A. Castineiras, Polyhedron 28 (2009) 3899–3906.
- [9] M. Belicchi-Ferrari, F. Bisceglie, E. Buluggiu, G. Pelosi, P. Tarasconi, Polyhedron 28 (2009) 1160–1168.
- [10] T.S. Lobana, S. Khanna, R. Sharma, G. Hundal, R. Sultana, M. Chaudhary, R.J. Butcher, A. Castineiras, Cryst. Growth Des. 8 (2008) 1203–1212.
- [11] A.D. Khalaji, G. Grivani, M. Rezaei, K. Fejfarova, M. Dusek, Phosphorus, Phosphorus Sulfur Silicon Relat. Elem. 188 (2013) 1119–1126.
- [12] E. Shahsavani, A.D. Khalaji, N. Feizi, M. Kucerakova, M. Dusek, Inorg. Chim. Acta 429 (2015) 61–66.
- [13] A.D. Khalaji, K. Fejfarova, M. Dusek, J. Cryst. Miner. 21 (2013) 1–4.
- [14] Y.M. Chumakov, N.M. Samus, G. Bocelli, K.Y. Suponitskii, V.I. Taspkov, A.P. Gulya, Russ. J. Coord. Chem. 32 (2003) 14–20.
- [15] L. Palatinus, G. Chapuis, J. Appl. Crystallogr. 40 (2007) 786–790.
- [16] V. Petricek, M. Dusek, L. Palatinus, Z. Kristallogr. 229 (2014) 345–352.
- [17] Diamond - Crystal and Molecular Structure Visualization. Crystal Impact - K. Brandenburg & H. Putz GbR, Rathausgasse 30, D-53111 Bonn.
- [18] K. Alomar, A. Landreau, M. Kempf, M.A. Khan, M. Allain, G. Bouet, J. Inorg. Biochem. 104 (2007) 397–404.
- [19] T.S. Lobana, R. Sharma, R.J. Butcher, Polyhedron 28 (2009) 1103–1110.
- [20] M. Hakimi, H. Vahedi, M. Rezvaninezhad, E. Schuh, F. Mohr, J. Sulf. Chem. 32 (2011) 55–61.
- [21] L.J. Ashfield, A.R. Cowley, J.R. Dilworth, P.S. Donnelly, Inorg. Chem. 43 (2007) 4121–4123.
- [22] E. Shahsavani, N. Feizi, V. Eigner, M. Dusek, A.D. Khalaji, J. Struct. Chem. 56 (2015) 103–107.
- [23] A.D. Khalaji, E. Shahsavani, N. Feizi, M. Kucerakova, M. Dusek, R. Azandarani, A. Amiri, C. R. Chim. (2016), <http://dx.doi.org/10.1016/j.crci.2016.05.009>.
- [24] M.I. Khan, A. Khan, I. Hussain, M.A. Khan, S. Gul, M. Iqbal, I. Ur-Rahman, F. Khuda, Inorg. Chem. Commun. 35 (2013) 104–109.